The anticonvulsant retigabine suppresses neuronal Kv2-mediated currents

Stas, Jeroen I; Bocksteins, Elke; Jensen, Camilla S; Schmitt, Nicole; Snyders, Dirk J

Published in:
Scientific Reports

DOI:
10.1038/srep35080

Publication date:
2016

Document version
Publisher's PDF, also known as Version of record

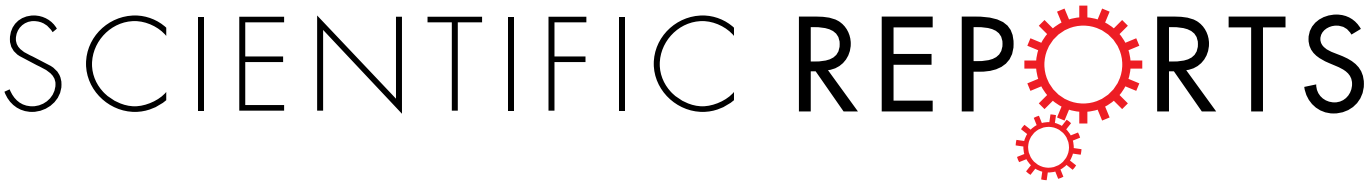

OPEN

The anticonvulsant retigabine suppresses neuronal K_V2-mediated currents

Received: 15 July 2016
Accepted: 20 September 2016
Published: 13 October 2016

Jeroen I. Stas[1,2], Elke Bocksteins[1], Camilla S. Jensen[2], Nicole Schmitt[2] & Dirk J. Snyders[1]

Enhancement of neuronal M-currents, generated through $K_V7.2$-$K_V7.5$ channels, has gained much interest for its potential in developing treatments for hyperexcitability-related disorders such as epilepsy. Retigabine, a K_V7 channel opener, has proven to be an effective anticonvulsant and has recently also gained attention due to its neuroprotective properties. In the present study, we found that the auxiliary KCNE2 subunit reduced the $K_V7.2$-$K_V7.3$ retigabine sensitivity approximately 5-fold. In addition, using both mammalian expression systems and cultured hippocampal neurons we determined that low μM retigabine concentrations had 'off-target' effects on $K_V2.1$ channels which have recently been implicated in apoptosis. Clinical retigabine concentrations (0.3–3 μM) inhibited $K_V2.1$ channel function upon prolonged exposure. The suppression of the $K_V2.1$ conductance was only partially reversible. Our results identified $K_V2.1$ as a new molecular target for retigabine, thus giving a potential explanation for retigabine's neuroprotective properties.

Epilepsy is a complex, debilitating neurological disorder affecting ~1% of the world's population. Currently, management of epileptic seizures consists of pharmacotherapy; however, in ~20–30% of patients, seizure control cannot be achieved with conventional treatment strategies[1,2]. In addition, in many cases drug-resistant epilepsy develops upon prolonged use of antiepileptic drugs (AED's). These drawbacks have fueled the search for non-conventional treatments and the development of more efficient pharmacotherapy in patients with refractory epilepsy[3–5].

Retigabine (RTG) is a novel, 'first-in-class' anticonvulsant drug approved for use in partial-onset seizures[6,7]. Unlike classical AED's that mainly affect voltage-gated Na^+ (Na_V) channels or NMDA/GABA-neurotransmission, retigabine primarily targets voltage-gated K^+ channels[1,2]. Retigabine selectively enhances the low treshold, non-inactivating neuronal M-current that regulates spike frequency adaptation and repetitive firing[6,8,9]. The molecular components of the M-current are the $K_V7.2$-$K_V7.5$ subunits encoded by *KCNQ2–5* genes respectively. Accordingly, many mutations in the *KCNQ2* and *KCNQ3* genes give rise to distinct epileptic phenotypes further underlining the significance of M-current's in regulating neuronal excitability[10–15]. Retigabine activates K_V7 channels by interfering with the normal gating behavior, i.e. retigabine shifts the voltage-dependence of activation to hyperpolarized potentials[16]. As a consequence, K_V7-mediated currents activate at more negative membrane potentials, effectively hyperpolarizing the resting membrane potential. The binding of retigabine to K_V7 channels occurs near the pore domain and is dependent on a conserved Trp residue ($K_V7.2$ Trp236) that is absent in the $K_V7.1$ channel primarily expressed in cardiac and epithelial cells[17,18]. More recently, it was found that the binding of retigabine is dependent on the hydrogen-bonding capability of the indole nitrogen atom in the Trp residue and the amide carbonyl oxygen atom of retigabine[19].

This general mechanism for suppression of neuronal excitability additionally makes retigabine and other K_V7 activators interesting compounds for several other hyperexcitability-related disorders such as migraine, chronic pain, tinnitus, and even Huntington's disease[20–23]. In addition, it has been shown that retigabine has neuroprotective properties[24–26]. However, not all of retigabine's effects are necessarily due to its action on K_V7 channels since it also modulates $GABA_A$ receptors in a similar concentration range[27]. Due to multiple case reports of long-term toxicity, its clinical application is now restricted to patients for whom other anticonvulsant drugs have proved inadequate[28–30]. Whether this toxicity arises from off-target retigabine receptors or chronic activation of K_V7

[1]Laboratory for Molecular Biophysics, Physiology and Pharmacology, Department of Biomedical Sciences, University of Antwerp, CDE, Universiteitsplein 1, 2610 Antwerp, Belgium. [2]Ion Channel Group, Department of Biomedical Sciences, University of Copenhagen, Blegdamsvej 3, DK-2200 Copenhagen N, Denmark. Correspondence and requests for materials should be addressed to D.J.S. (email: dirk.snyders@uantwerpen.be)

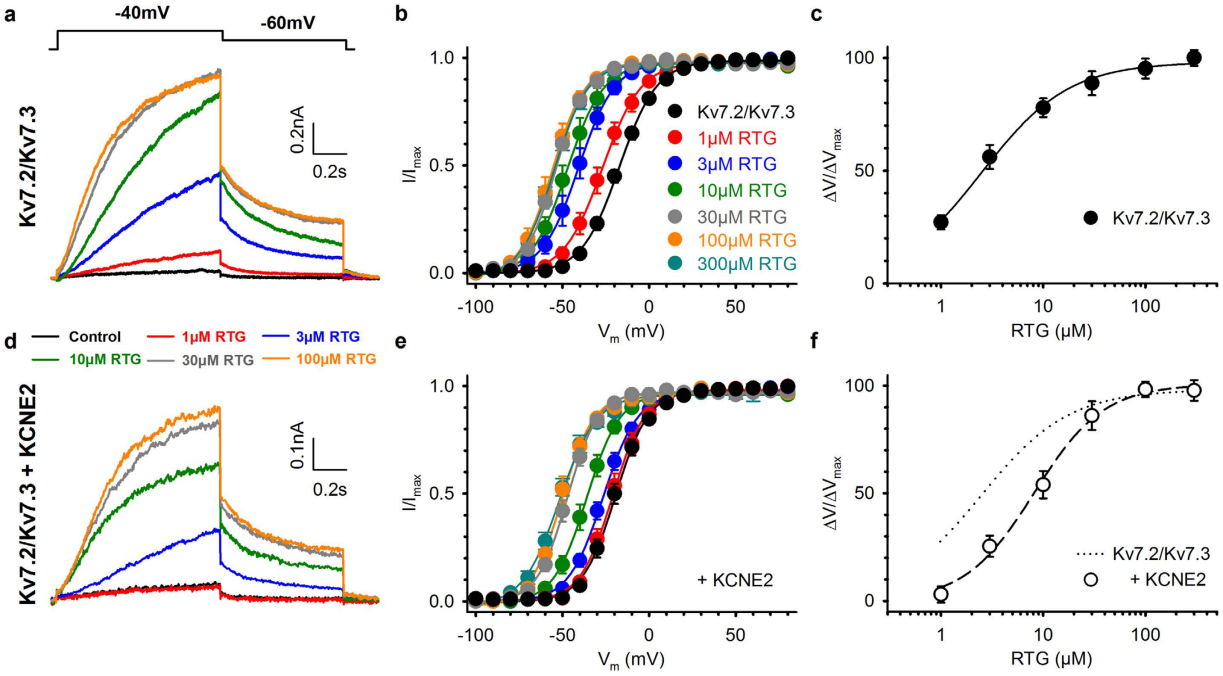

Figure 1. KCNE2 decreases the retigabine sensitivity of heterotetrameric $K_V7.2$-$K_V7.3$ channels. (**a**) Effect of increasing concentrations of retigabine (1–100 μM) on $K_V7.2$-$K_V7.3$ currents. Retigabine potentiated the $K_V7.2$-$K_V7.3$ current in a concentration-dependent manner, and saturation occurred above 30 μM. Voltage protocol is shown on top. (**b**) Voltage-dependence of activation. Increasing concentrations of RTG caused a gradual hyperpolarizing shift. (**c**) Concentration-effect curve plotted as the shift in the voltage-dependence of activation normalized to the maximal observed shift ($\Delta V/\Delta V_{max}$) as function of the drug concentration. (**d**) Similar to (**a**) but after co-expression with KCNE2. Retigabine potentiated the $K_V7.2$-$K_V7.3$-KCNE2 currents but unlike (**a**) concentrations above 1 μM had to be used. (**e**) Voltage-dependence of activation. KCNE2 reduced the hyperpolarizing shift at every drug concentration, and decreased the maximal observed shift (ΔV_{max}). (**f**) Concentration-effect curve.

channels remains unknown. Surprisingly, despite the large structural similarities within the K_V channel family, little effort has been made to determine whether other K_V channels are modulated by retigabine[7]. In addition to this, it has not yet been investigated whether the accessory subunit KCNE2 impacts the retigabine effect on K_V7 despite the fact that $K_V7.2$-$K_V7.3$ channels and KCNE2 have overlapping expression patterns and described gating effects[31,32].

Here, we performed an electrophysiological screening on members of the K_V1–K_V9 and K_V11 subfamilies to investigate whether these channels are affected by retigabine. We found that retigabine inhibited all K_V channels tested, but that this inhibition only occurred in the high μM range, with the exception of $K_V2.1$. Inhibition of $K_V2.1$ required only low μM concentrations and was only partially reversible. In addition, we found that the addition of the auxiliary subunit KCNE2 decreased the retigabine sensitivity of heterotetrameric $K_V7.2$-$K_V7.3$, but not of $K_V2.1$, channels. These findings identify $K_V2.1$ as an important molecular target for the action of retigabine and, due to $K_V2.1$'s key role in apoptosis, could help explain the previously reported neuroprotective properties[24–26].

Results

KCNE2 modulates retigabine sensitivity of $K_V7.2$-$K_V7.3$ channels. The pharmacology of K_V7 channels is highly dependent on its association with auxiliary KCNE subunits[33,34]. Of the five known KCNE proteins, KCNE2 potentially interacts with the main determinants of the M-current - heteromeric $K_V7.2$-$K_V7.3$ channels - based on overlapping expression patterns and gating effects[31,32]. Hence, we co-transfected $K_V7.2$-$K_V7.3$ with YFP-KCNE2 enabling us to select KCNE2-transfected cells. Retigabine potentiated $K_V7.2$-$K_V7.3$ currents in a concentration-dependent manner (Fig. 1a) by shifting the voltage-dependence of activation to hyperpolarized potentials (Fig. 1b) with an EC_{50} of 1.9 ± 0.3 μM and a Hill coefficient of 1.4 ± 0.1 ($n = 11$; Fig. 1c), as previously reported[7,16,17]. Co-transfection of KCNE2 with the $K_V7.2$-$K_V7.3$ channel complexes did not prevent retigabine from potentiating the current (Fig. 1d). However, KCNE2 reduced the shift in the voltage-dependence of activation (ΔV) at every concentration (Fig. 1e), resulting in a right-shifted concentration-effect curve with an EC_{50} of 10.0 ± 2.2 μM and a Hill coefficient of 1.0 ± 0.1 ($n = 9$; Fig. 1f). In addition, the maximal shift in the voltage-dependence of activation (ΔV_{max}) was reduced from 39.2 ± 1.4 mV ($n = 11$) under control conditions to 30.7 ± 1.1 mV ($n = 9$) in the KCNE2-transfected cells (see Supplementary Table S1). Thus, KCNE2 reduced the retigabine sensitivity of $K_V7.2$-$K_V7.3$ channels approximately 5-fold.

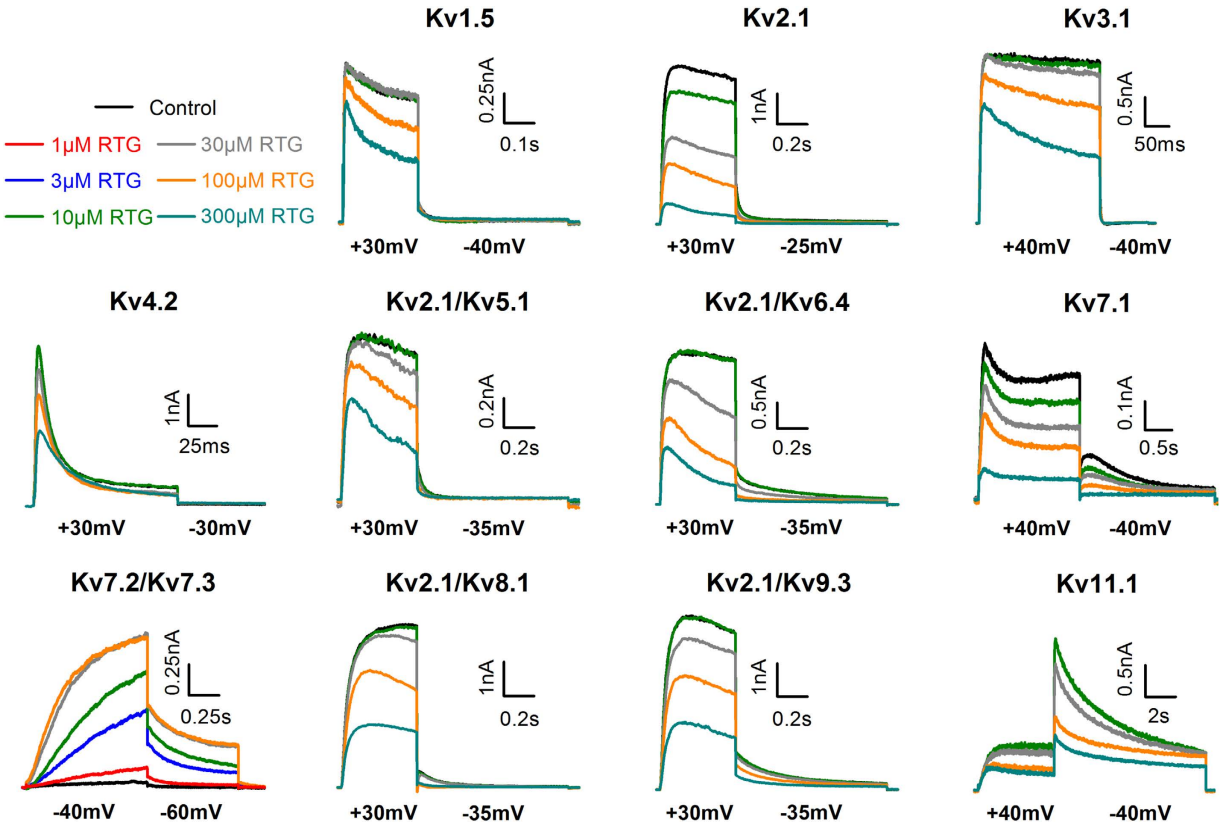

Figure 2. Retigabine inhibits most K_V channels in the intermediate to high μM range. A two-step pulse protocol adjusted to the biophysical properties of the respective channel was used. The voltage applied is shown below the respective K_V channel current traces. Retigabine (colored traces) inhibited all K_V channels in the high μM range (>100 μM) with exception of K_V2.1, which was inhibited at relative low μM concentrations (10 μM).

Retigabine inhibits K_V channels. To determine whether retigabine affected other Kv channels, we screened representative channels of the K_V1–K_V9 and K_V11 subfamilies (Fig. 2). A two-step screening pulse adjusted to the biophysical properties of the respective channel was used. Since they cannot form homotetrameric channels at the plasma membrane, members of the K_V5, K_V6, K_V8, and K_V9 subfamilies where co-transfected with K_V2.1[35]. Retigabine inhibited all K_V channels tested, though only at high μM concentrations (>100 μM). However, K_V2.1 currents were inhibited at relatively low concentrations (10 μM) (Fig. 2). Interestingly, this increased sensitivity was absent when K_V2.1 co-assembled respectively with K_V5.1, K_V6.4, K_V8.1, and K_V9.3 subunits.

K_V2.1 inhibition is voltage-dependent and only partially reversible. To gain insight into the underlying mechanism of K_V2.1 channel inhibition, we performed a detailed biophysical characterization of retigabine effects. Retigabine inhibited K_V2.1 currents with an IC_{50} of 22.0 ± 1.6 μM and Hill coefficient of 1.6 ± 0.1 (n = 5; Fig. 3b). Although KCNE2 was previously found to interact with K_V2.1[33], it did not alter the IC_{50} for inhibition. Retigabine inhibition of K_V2.1-KCNE2 currents occurred with an IC_{50} of 16.1 ± 1.8 μM (p = 0.056) and a Hill coefficient of 1.4 ± 0.2 (p = 0.384) (n = 6). No change could be observed in the voltage-dependence of inactivation (triangles, Fig. 3c) or the time constants of channel opening/closing (Fig. 3d). However, retigabine did induce a small but significant hyperpolarizing shift of approximately 6 mV (p = 0.012), from 3.7 ± 1.5 (n = 12) to −2.5 ± 1.6 mV (n = 9), in the voltage-dependence of activation (circles, Fig. 3c and Table 1). Next, we determined the voltage-dependence of channel inhibition (or fractional inhibition), obtained by dividing the current-voltage (I-V) relationships in Fig. 3e, and plotted this alongside the voltage-dependence of activation (Fig. 3f). Inhibition of K_V2.1 displayed a clear voltage-dependency; less inhibition occurred at weak depolarizing potentials where only a small fraction of K_V2.1 channels conducted current. 100 μM retigabine inhibited 78.0 ± 3.4% (n = 7) of the current at +60 mV while only 27.0 ± 12.4% (n = 7) inhibition occurred at −10 mV (Fig. 3f).

Furthermore, we determined the wash-in/wash-out kinetics of K_V2.1 channel inhibition at +30 mV where the voltage-dependence of inhibition was maximal (see Fig. 3f). Inhibition of K_V2.1 currents was only partially reversible and appeared to accelerate the development of channel inactivation, indicating an open-channel block mechanism (Fig. 4a). Inhibition of K_V2.1 by 100 μM retigabine was slow, with a $\tau_{wash\text{-}in}$ of 89.7 ± 14.4 s (n = 10), on average requiring ± 10 minutes before inhibition was saturated (Fig. 4b). Recovery of inhibition was markedly slower, with a $\tau_{wash\text{-}out}$ of 574 ± 67 s (n = 8), and incomplete with only 41.8 ± 7.6% recovery in 30 minutes (Fig. 4d and Table 1). Recovery of inhibition was significantly different from normal rundown (p < 0.001) and was not dependent on the solvent: addition of 1% DMSO did not increase the rate of recovery (Fig. 4c). Next, we

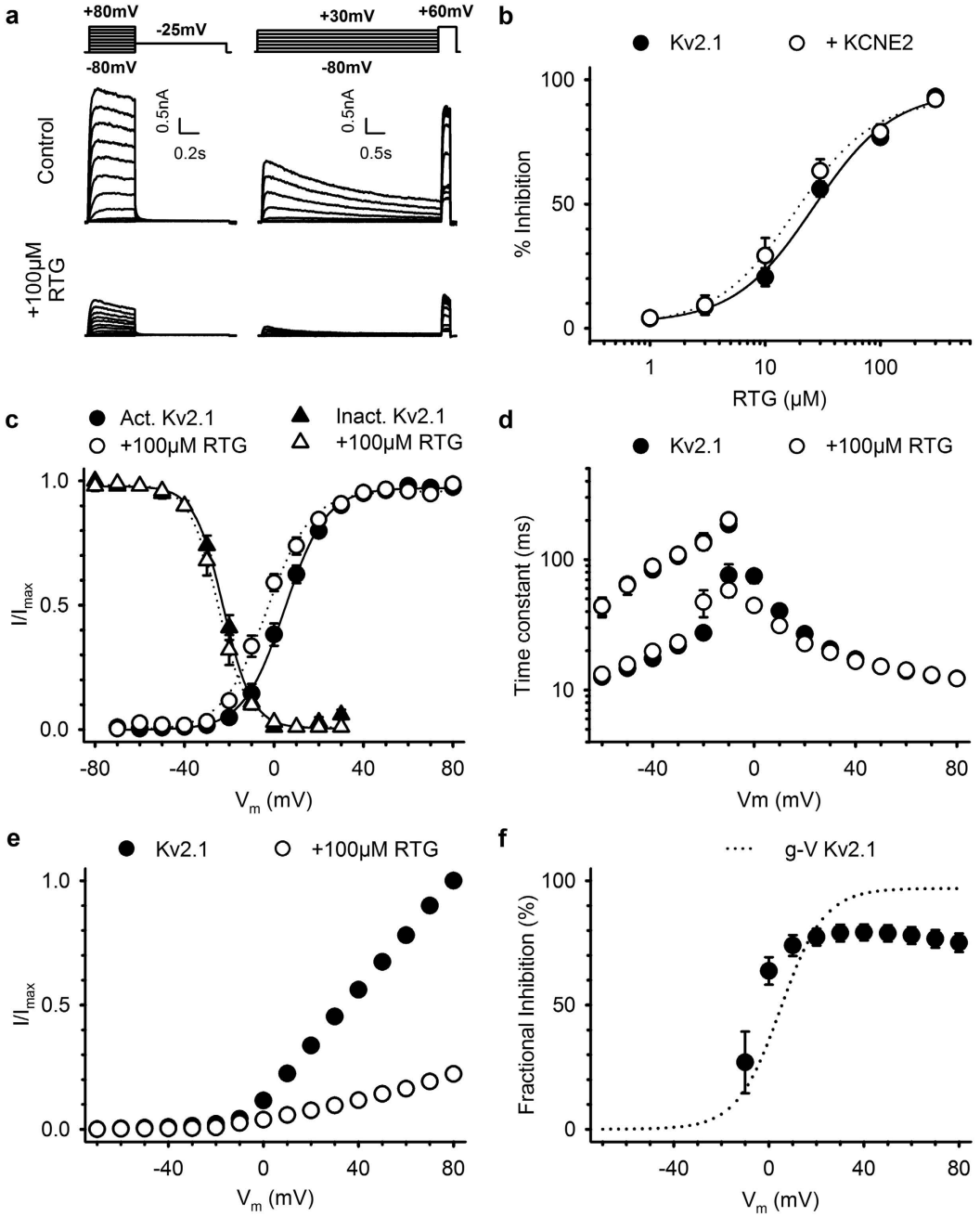

Figure 3. Retigabine inhibition of $K_V2.1$ is voltage-dependent. (**a**) Typical current recordings of $K_V2.1$ channels to determine the activation (left) and inactivation (right) properties, before (top) and after exposure to 100 μM retigabine (bottom). Voltage protocols are shown on top. (**b**) Concentration-effect relationship of $K_V2.1$ inhibition. Retigabine inhibition of $K_V2.1$ (closed circles) currents was not significantly different ($p = 0.385$) in the presence of KCNE2 (open circles). (**c**) Voltage-dependence of activation (circles) and inactivation (triangles) in absence (closed symbols) and presence (open symbols) of 100 μM retigabine. The voltage-dependence of activation was obtained by plotting the normalized tail currents (I/I_{max}) in the activation current traces from panel A as function of the prepulse potential. Retigabine induced a small but significant ($p = 0.012$) hyperpolarizing shift in the voltage-dependence of activation. The voltage-dependence of inactivation, obtained by plotting the normalized peak current (I/I_{max}) at +60 mV after a 5 s prepulse as a function of the prepulse potential, was not affected by retigabine. (**d**) Time constants of $K_V2.1$ channel opening (≥0 mV) and closing (<0 mV) in absence (filled circles) and presence (open symbols) of 100 μM retigabine. (**e**) Current-voltage (I-V) relationship, obtained by plotting the current at the end of the 500 ms varying pulse as function of the voltage. (**f**) Fractional inhibition as function of the applied voltage. The fractional inhibition, obtained by dividing the I-V relationships in (**e**) displayed significantly less inhibition at weak depolarizing potentials. The dotted line represents the voltage-dependence of activation of $K_V2.1$.

	Activation			Inactivation		
	$V_{1/2}$	k	n	$V_{1/2}$	k	n
K_V2.1	3.7 ± 1.5	8.7 ± 0.4	12	−21.8 ± 1.0	6.2 ± 0.3	7
100 μM RTG	−2.5 ± 1.6	10.0 ± 1.4	9	−24.2 ± 1.6	5.9 ± 0.4	10
RTG incubation						
Control	3.8 ± 1.0	9.0 ± 0.5	14	−21.4 ± 2.6	5.4 ± 0.2	5
0.1% DMSO	1.9 ± 1.8	8.3 ± 0.3	11	−22.8 ± 3.0	5.60.2	5
0.1 μM RTG	4.9 ± 1.0	8.8 ± 0.3	12			
0.3 μM RTG	3.9 ± 1.5	8.8 ± 0.5	13			
1 μM RTG	6.3 ± 1.6	8.9 ± 0.6	12	−17.0 ± 1.5	5.8 ± 0.4	5
3 μM RTG	6.7 ± 1.2	8.0 ± 0.4	12			
Inhibition Kinetics						
	$\tau_{wash\text{-}in}$ (s)	**$\tau_{wash\text{-}out}$ (s)**		**% Inhibition**	**% Recovery**	**n**
100 μM RTG	89.7 ± 14.4	574 ± 67		80.8 ± 2.7	41.8 ± 7.6	8

Table 1. Biophysical properties of K_V2.1. $V_{1/2}$, midpoint of activation or inactivation; k, slope factor; n, number of cells; $\tau_{wash\text{-}in}$, the rate of inhibition; $\tau_{wash\text{-}out}$, the rate of recovery. Values significantly different from the control values are shown in bold ($p < 0.05$).

investigated the state-dependence of inhibition to determine whether retigabine was capable of inhibiting K_V2.1 channels in their closed-state (Supplementary Fig. S1a). Application of retigabine during a 300 s pulse to −90 mV (where all channels are closed) inhibited the peak and 'end' current at a test pulse to +30 mV compared to the control (Supplementary Fig. S1a,b). However, subsequent recording of a train of pulses revealed that this degree of inhibition was significantly different from saturated inhibition. Interestingly, during the 'conventional' wash-in experiments the inhibition saturated within 300 s (Fig. 4b). Thus, these observations argue against efficient inhibition of closed K_V2.1 channels by retigabine. Evidence for this inefficient inhibition of closed K_V2.1 channels was further strengthened when we compared the 'peak' and 'end' currents of the wash-in protocols illustrated in Fig. 4b (Supplementary Fig. S1c), The 'peak' current during the next step was always 10–15% larger than at the end of the previous pulse. This indicates that no significant additional inhibition developed during the 14.5 s interval at −80 mV. Given the similar 'recovery' independent of the level of inhibition, this most likely reflects recovery from slow inactivation at −80 mV.

The slow onset of inhibition combined with the incomplete recovery raised the question whether clinically relevant concentrations of retigabine could affect K_V2.1 when the exposure time was increased. To investigate this, we performed 'incubation' experiments (illustrated in Supplementary Fig. S2a). HEK cells were transfected and exposed to low concentrations of retigabine (0.1–3 μM) for 4 hours. Interestingly, retigabine reduced the K_V2.1 current density in a concentration-dependent manner, independent of the manipulation or solvent (Supplementary Fig. S2b). The current density was significantly reduced by approximately 2.5-fold after exposure to 1 ($p = 0.027$) and 3 μM ($p = 0.024$) retigabine (Supplementary Fig. S2c). To exclude the possibility that the reduced current densities occurred as a consequence of altered K_V2.1 channel gating, we determined the voltage-dependence of activation for each condition, and found that it was not modified (Supplementary Fig. S2d). A full biophysical characterization was performed for control and exposure to 0.1% DMSO and 1 μM retigabine, but no significant changes were observed (data not shown).

Retigabine inhibits native K_V2.1 currents in rat hippocampal neurons. To determine whether the inhibition observed in an overexpression system translated to similar effects in an *in vivo* setting, we tested native K_V2-mediated currents in cultured rat hippocampal neurons. Total outward currents were recorded with a prepulse to −10 mV to eliminate most of the I_A current, as previously described[36]. 100 μM retigabine was used for this purpose because: 1) it caused significant inhibition of K_V2-mediated currents and 2) did not substantially inhibit other K_V channels (see Fig. 2). The degree of inhibition was determined at the end of the 250 ms pulse. As expected, retigabine caused significant inhibition, 44.0 ± 3.2% at +60 mV ($n = 9$), of the total outward current in cultured rat hippocampal neurons (Fig. 5a). To further identify the retigabine inhibited currents as K_V2.1-mediated, we used Guangxitoxin-1E (GxTx-1E), a selective Kv2 inhibitor[37]. We used a concentration of 100 nM GxTx-1E that has been reported to produce near-saturating effects on K_V2-mediated currents in mice CA1 hippocampal neurons[37]. GxTx-1E caused little additional inhibition (8.2 ± 4.8%, $n = 6$ and $p = 0.146$) of the total outward current suggesting that retigabine inhibited the majority of K_V2-mediated currents. To validate these results, we performed the experiments in the reverse order: K_V2-mediated currents were first inhibited with GxTx-1E, before retigabine was applied (Fig. 5b). GxTx-1E inhibited 45.7 ± 2.0% ($n = 6$) of the total outward current at +60 mV and retigabine did not cause significant additional inhibition (6.9 ± 3.6%, $n = 6$ and $p = 0.589$). As an additional control, we repeated the experiments with 5 μM tetrodotoxin (TTX) in the bathing solution, in order to block Na_V channels (Supplementary Fig. S3). Retigabine still inhibited a major component of the total outward current in the presence of extracellular TTX, with little additional inhibition caused by GxTx-1E ($n = 3$)(Supplementary Fig. S3a). The normalized current-voltage relationships confirmed these observations. When K_V2-mediated currents were not first inhibited with GxTx-1E, retigabine inhibited a major component of the total outward current (Fig. 5c,d and Supplementary Fig. S3c). Interestingly, as observed for the retigabine

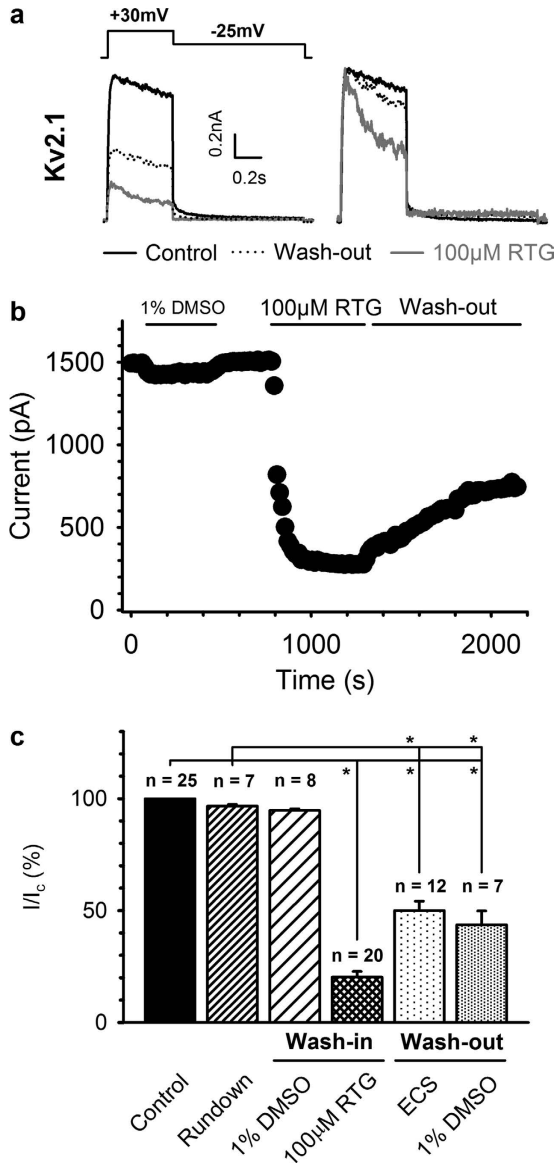

Figure 4. Inhibition of $K_V2.1$ current by retigabine is only partly reversible. (**a**) Representative $K_V2.1$ current traces (black) at +30 mV (left). The scaled current traces are shown in the right panel. Retigabine (grey) inhibited approximately 80% of the current but inhibition was poorly recovered 30 minutes after removal of retigabine (dotted). The 'apparent' acceleration of the inactivation process seen in the scaled current traces most likely reflects open-channel block by retigabine. (**b**) Plot of a representative wash-in/wash-out experiment. Inhibition of the $K_V2.1$ current occurred slowly, typically requiring 5–10 minutes to achieve saturation. Inhibition of $K_V2.1$ currents was poorly reversible and occurred extremely slow. (**c**) Bar chart illustrating the degree of current (I/I_c), with I the current at a given condition and I_c the control condition. $K_V2.1$ inhibition was poorly reversible, independent of the solvent, and significantly different from current rundown. *Indicates statistical significance ($p < 0.05$).

inhibition of $K_V2.1$ in HEK cells, retigabine inhibited the total outward current in a voltage-dependent manner with decreased sensitivity at weak depolarizing potentials.

Discussion

Enhancement of K_V7 channel activity by retigabine provides a general mechanism for suppression of multiple hyperexcitability-related disorders such as epilepsy, chronic pain and tinnitus[20–22]. Our results illustrate that the auxiliary KCNE2 subunits reduced the retigabine sensitivity of $K_V7.2$-$K_V7.3$ by approximately 5-fold. Although the role of KCNE2 in the nervous system and its interaction with $K_V7.2$-$K_V7.3$ channels remain controversial, the potential of KCNE2 to modulate K_V channel pharmacology is well established[31,33]. The interaction between KCNE2 and $K_V7.2$-$K_V7.3$ channels alters the biophysical properties modestly[32]. Our study showed that KCNE2 reduced the retigabine sensitivity of $K_V7.2$-$K_V7.3$ channels, further supporting the idea that KCNE2 can interact with these $K_V7.2$-$K_V7.3$ channels. However, we did not observe the previously reported KCNE2-induced

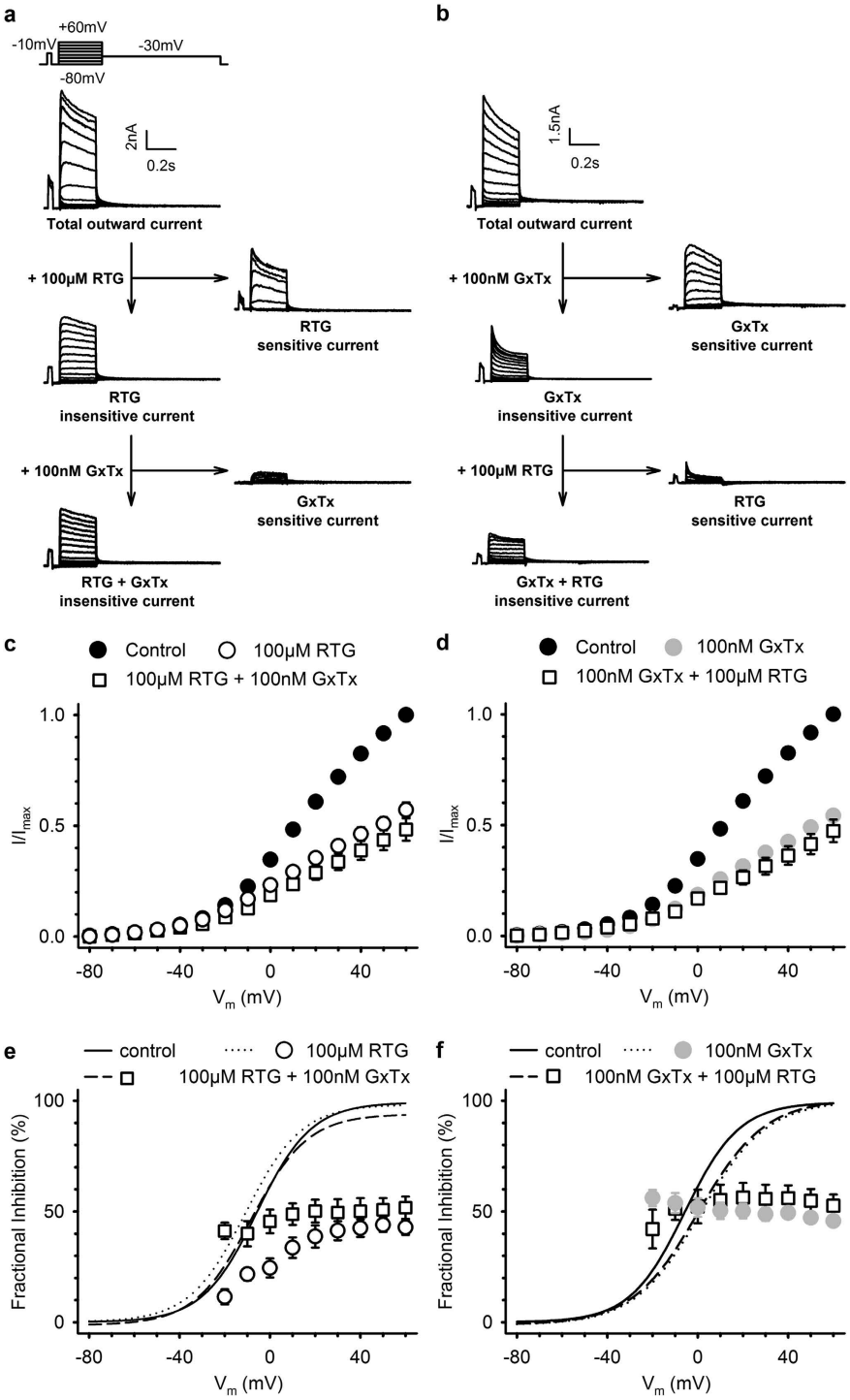

Figure 5. Retigabine inhibits the K_V2-mediated component of the outward current in cultured rat hippocampal neurons. (**a**) Representative current traces from cultured rat hippocampal neurons. 100 μM retigabine inhibited the outward current and the RTG-sensitive current was obtained after subtraction. 100 nM Guangxitoxin-1E (GxTx), i.e. selective K_V2 inhibitor, was used to confirm the inhibition of K_V2-mediated current by retigabine. Retigabine inhibited a major component of delayed rectifier current, with little inhibition caused by GxTx (**b**) similar to (**a**) although the K_V2-mediated current was first inhibited with GxTx before applying retigabine. Inhibition of the K_V2-mediated component of the current by GxTx resulted in little inhibition of retigabine. However, retigabine still inhibited a fast activating and inactivating current. (**c,d**) Current-voltage relationship, obtained by plotting the total outward current at the end of the 250 ms step as function of the voltage with retigabine (**c**) or GxTx (**d**) initial exposure. (**e,f**) Fractional inhibition as a function of the applied voltage. As observed in HEK cells (Fig. 3f), retigabine (**e**) had a voltage-dependence of inhibition that could be abolished after subsequent exposure to GxTx. Panel (**f**) is similar to (**e**) but with initial exposure to GxTx. Lines represent the voltage-dependence of activation fitted with the Boltzmann equation.

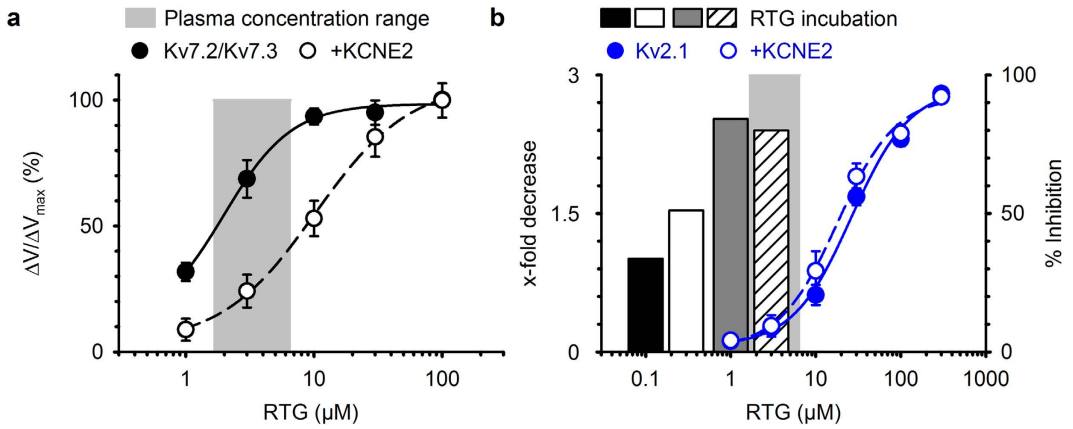

Figure 6. Molecular pharmacology on K_V2 and K_V7 channels in HEK cells compared with retigabine plasma concentrations. (**a**) Concentration-effect relationship of retigabine potentiation on $K_V7.2$-$K_V7.3$ currents in the absence (filled circles) and presence (open circles) of KCNE2. The grey bar represents the plasma concentration range, minimum (0.65 μM) to maximum (6.6 μM), in patients treated with 600–1200 mg retigabine/day[38–42]. Although KCNE2 shifted the concentration-effect curve, $K_V7.2$-$K_V7.3$ current potentiation was not fully prevented in the plasma concentration range. (**b**) Concentration-effect relationship of $K_V2.1$ inhibition in absence (blue, filled circles) and presence (blue, open circles) of KCNE2, obtained from direct perfusion of retigabine on the Kv2.1 channels. The light grey bar represents the plasma concentration range as in (**a**). Black, white, dark grey and striped bar represent the x-fold reduction in $K_V2.1$ current density obtained from the retigabine incubation experiments. Although little direct $K_V2.1$ inhibition occurred, maximal suppression of the $K_V2.1$ current density occurred in the plasma concentration range.

changes in the biophysical properties. In our experiments, KCNE2 had the tendency to hyperpolarize the voltage-dependence of activation. Even though KCNE2 reduced the retigabine sensitivity of $K_V7.2$-$K_V7.3$ channels, it still had some effect within the clinical plasma concentration range as illustrated in Fig. 6a where we show the concentration-effect curves together with the retigabine plasma concentration range[6,38–42].

By demonstrating that clinically relevant retigabine concentrations inhibited K_V2-currents, presumably through an open channel block mechanism, both in HEK cells and hippocampal neurons (Fig. 6b), our findings indicate that K_V2 channels might represent an important 'off-target' receptor responsible for some of retigabine's (adverse) effects. Although acute exposure of $K_V2.1$ channels to retigabine resulted in inhibition at concentrations above the clinical range (blue circles Fig. 6b), the prolonged incubation experiments (bars Fig. 6b) revealed a strong reduction of the $K_V2.1$ current density at clinical, and even sub-clinical concentrations of retigabine. As a result, retigabine might exert a significant effect on $K_V2.1$ channels *in vivo*. Pharmacological suppression of K_V2 channels results in either an increase or decrease of neuronal excitability, as previously shown with the K_V2-selective inhibitor GxTx-1E[37]. GxTx-1E inhibits between 60–80% of the total delayed rectifier current in rat superior cervical ganglion neurons and mouse hippocampal CA1 neurons. This results in an increased initial firing frequency but depresses maintained firing. 100 nM GxTx-1E only inhibited ~50–55% of total outward current in our experiments. This discrepancy most likely arises from differences in the age of the hippocampal neurons used: Liu and Bean performed recordings on acutely dissociated hippocampal neurons while our recordings were performed on hippocampal neurons that were cultured for 10–15 days *in vitro*.

$K_V2.1$ channel expression is rather ubiquitous and serves major physiological functions in the central nervous system and (neuro)endocrine cells[43,44]. $K_V2.1$ channels constitute the major delayed rectifier current in hippocampal neurons, and targeted deletion of $K_V2.1$ results in neuronal and behavioral hyperexcitability[37,45,46]. The expression pattern of $K_V2.1$ channels is intriguing, in that they form cell-surface clusters at the soma, proximal dendrites and the axon initial segment, not only in cultured hippocampal neurons and intact brain but also in transfected HEK cells[47,48]. Interestingly, within the clusters, $K_V2.1$ channels are inactive, i.e. gating charge movement of the voltage sensing domains was detected without measurable ionic currents, and upon dispersal, the ionic current is regained. Within the micro-domain of the cluster, $K_V2.1$ channels are in close proximity to the endoplasmatic reticulum (ER) and induce the formation of ER-plasmamembrane junctions[49–51]. Thus, it was suggested that $K_V2.1$ cell surface clusters are insertion platforms for ER-membrane trafficking[52]. Clustering of $K_V2.1$ is highly dependent on the phosphorylation state of the channel and directly linked to underlying neuronal activity. This means that hyperexcitability, as observed during epileptic seizures, promotes dephosphorylation of $K_V2.1$ through a Ca^{2+}/calcineurin-dependent mechanism which leads to increased $K_V2.1$ activity and $K_V2.1$ declustering[36,53,54]. Interestingly, $K_V2.1$ clusters can also be dispersed pharmacologically. When hippocampal neurons are exposed to glutamate, rapid $K_V2.1$ declustering occurs[55]. Due to the fact that retigabine inhibited $K_V2.1$ currents in a poorly reversible manner, both in HEK cells and hippocampal neurons, $K_V2.1$ trafficking might be affected upon retigabine exposure. One could speculate that loss of functional $K_V2.1$ channels at the cell surface, due to increased endocytosis or changed clustering pattern, might contribute to retigabine's poorly reversible inhibition of Kv2.1 currents. However, using live-cell imaging of GFP-tagged $K_V2.1$, we did not observe a change in the $K_V2.1$ localization within 30 min after exposure to retigabine (data not shown). Interestingly, $K_V2.1$ current

densities were reduced with much lower retigabine concentrations (0.1–3 μM) upon prolonged exposure. In this case, the reduced $K_V2.1$ current density might simply reflect the population of $K_V2.1$ channels that were not inhibited by retigabine as the gating and trafficking (data not shown) properties were not modified. In addition, it cannot be excluded that the observed reduction in $K_V2.1$ current density is (partially) caused by a drug metabolite of retigabine. On the other hand, retigabine's hydrophobic nature suggests that it might reside in the lipid bilayer or bind to a hydrophobic region in the $K_V2.1$ channel. Although this could help explain the poor reversibility of $K_V2.1$ current inhibition upon wash-out, it seems rather unlikely, because: 1) increased solvent concentrations had no significant effect on the reversibility of inhibition (Fig. 4c), and 2) retigabine's action on K_V7 channels was always fully reversible. An interesting future direction will be to further investigate the underlying mechanism of this poorly reversible reduction in $K_V2.1$ current densities.

Interestingly, $K_V2.1$ might be involved in the neuroprotective properties of retigabine that have been described more recently, especially due to the key role of $K_V2.1$ in apoptosis[56,57]. Upon neuronal injury, $K_V2.1$-currents are increased through *de novo* insertion of channels in the plasma membrane and subsequent decrease of intracellular $[K^+]$ levels promoting activation of the apoptotic cascade[58]. The extent of cell death can be reduced when the pro-apoptotic $K_V2.1$ current is pharmacologically inhibited[59]. Therefore, retigabine might prevent apoptosis through inhibition of $K_V2.1$ currents, thus promoting cell survival. However, retigabine was found to promote neuroprotection by diminishing excitotoxicity through suppression of hyperexcitability by K_V7 channel activation[24–26]. Thus, retigabine might promote neuroprotection in neurons through its concerted action on K_V2 and K_V7 channels.

In conclusion, we found that the retigabine sensitivity of K_V7 channels is reduced by the auxiliary KCNE2 subunit. In addition, retigabine inhibited $K_V2.1$ channels most likely through an open-channel block mechanism in a poorly reversible manner at clinically relevant concentrations.

Materials and Methods

Molecular biology. Human $K_V1.5$ (GenBank Accession Number NM_002234), $K_V2.1$ (NM_004975), $K_V3.1$ (NM_004976), $K_V4.2$ (NM_012281), $K_V5.1$ (NM_002236), $K_V6.4$ (NM_172347), $K_V8.1$ (NM_014379) and $K_V11.1$ (NM_000238), as well as mouse $K_V9.3$ (NM_173417), were subcloned in the eGFP-N1 vector (Clontech, Palo Alto, CA, USA). Human $K_V7.1$ (NM_000218), $K_V7.2$ (NM_172107), $K_V7.3$ (NM_004519), KCNE2 (NM_172201) and YFP-KCNE2 were subcloned in the pBK/CMV vector as described previously[60].

Transient transfection and cell culture. HEK293 cells were cultured in 60 mm cell culture dishes filled with 4 ml culture medium - consisting of Dulbecco's modified Eagle's medium supplemented with 10% horse serum, 1% penicillin/streptomycin and 1% non-essential amino acids–under physiological conditions (37 °C and 5% CO_2). HEK293 cells were transiently transfected with 0.05–5 μg cDNA of the respective channel together with the GFP transfection marker using Lipofectamine2000 (Invitrogen, San Diego, CA, USA), according to the manufacturer's instructions. To obtain the characteristic $K_V7.2$-$K_V7.3$ currents both K_V subunits were co-transfected in a 1:1 molar ratio. Co-transfection with KCNE2 was performed in 1:1:4 and 1:4 molar ratios for $K_V7.2$-$K_V7.3$ and $K_V2.1$ channels, respectively. The amount of cDNA was kept identical between the–KCNE2 and +KCNE2 experiments by addition of empty vector cDNA. A C-terminal YFP-KCNE2 construct was used to allow for selection of KCNE2-transfected cells. The YFP-KCNE2 behaved similarly to the untagged KCNE2. 16–24 h after transfection, HEK293 cells were dissociated with trypsine and transferred to the patch-clamp set-up for electrophysiological analysis.

The retigabine incubation experiments were performed on HEK293 cells transfected with 10 ng $K_V2.1$ over 48 h. 24 h post-transfection, HEK293 cells were either exposed to normal medium (control) containing 0.1% DMSO (vehicle control) or 0.1, 0.3, 1 or 3 μM retigabine for 4 h. After the 4 h exposure, the incubation medium was removed and fresh medium was added to the transfected HEK293 cells. Thus, at the moment of electrophysiological analysis (48 h post-transfection), no retigabine was present in the recording solution.

Primary cultures of rat hippocampal neurons. All use of animals was approved by the institutional animal care and use committee of the University of Copenhagen. All experiments were performed in accordance with the relevant guidelines and regulations. Primary cultures of rat hippocampal neurons were obtained as described previously[61]. In summary, whole brains were removed from E18/E19 rat embryos. Hippocampi were dissected, and the cells dissociated and cultured on poly-L-lysine treated coverslips that were placed upon an astrocyte feeder layer. Hippocampal neurons were cultured 10–15 days *in vitro* and afterwards analyzed with the patch–clamp technique.

Electrophysiology. Whole-cell ionic currents were recorded as previously described[62]. In summary, whole-cell current recordings were performed at room temperature (20–22 °C) utilizing an Axopatch-200B/700B amplifier (Axon instruments, Union City, CA, USA), sampled at a 1–10 kHz frequency using a Digidata 1440/1550 acquisition system (Axon instruments) and filtered with a low-pass Bessel filter. The pClamp10 software (Axon instruments) controlled the command voltages and managed the data storage. HEK293 cells were continuously perfused with extracellular solution (ECS) containing (in mM): 145 NaCl, 4 KCl, 1 $MgCl_2$, 1 $CaCl_2$, 10 HEPES and 10 Glucose, adjusted to a pH of 7.35 with NaOH. Patch pipettes (1.5–2.5 MΩ) were pulled from borosilicate glass capillaries, heat polished and filled with an intracellular solution (ICS) containing (in mM): 110 KCl, 5 K_2ATP, 5 K_4BAPTA, 2 $MgCl_2$ and 10 HEPES, pH adjusted to 7.2 with KOH. ICS and ECS solutions were used to record in HEK293 cells as well as in native hippocampal neurons. Where mentioned, 5 μM TTX was added to the ECS solution to inhibit native Na^+ currents. When leak currents exceeded 10% of the total ionic current or voltage errors at the highest used potential exceeded the cut-off value of 5 mV (after series resistance compensation), cells were excluded from analysis.

Drug solutions. All drug solutions were applied to the HEK293 cells using a fast perfusion system (ALA scientific Instruments, Farmingdale, NY, USA). Control recordings were obtained with fast perfusion of ECS solution. Retigabine (Alomone Labs, Jerusalem, Israel) was dissolved in DMSO to obtain a stock solution of 100 mM. The working concentrations (0.1–300 μM) were obtained by diluting the stock solution in ECS solution. Guangxitoxin–1E (Alomone Labs) and TTX (Sigma-Aldrich, Schnelldorf, Germany) were dissolved and diluted in ECS solution to obtain the stock (100 μM and 5 mM) and working (100 nM and 5 μM) solutions.

Data analysis and statistics. The Hill equation: $1 - y = 1/(1 + (EC_{50}/[D])^{n}_{H})$, was fitted to concentration-effect curves to obtain a relative measurement of drug affinity with EC_{50} the concentration that induces 50% of the effect and n_H the Hill coefficient. For Kv7 channels the effect is defined as the induced shift in the voltage–dependence of activation normalized to the maximal shift (i.e. $\Delta V/\Delta V_{max}$) while for Kv2.1 the degree of current inhibition (%) was plotted. The Boltzmann equation: $y = 1/(1 + \exp(-(V - V_{1/2})/k))$, was applied to fit the voltage–dependence of (in)activation, where V represents the applied potential, $V_{1/2}$ the voltage where 50% of the channels are (in)activated, and k the slope factor. Results were reported as the mean value ± S.E.M. Standard t–test or the Mann–Whitney Rank Sum test were used to determine whether the results achieved statistical significance. Statistical significance was defined as $P < 0.05$. Pulse protocols were adjusted to match the biophysical properties of the respective Kv channel and are illustrated throughout the figures.

References

1. Bialer, M. & White, H. S. Key factors in the discovery and development of new antiepileptic drugs. *Nat. Rev. Drug Discov.* **9,** 68–82 (2010).
2. Loscher, W., Klitgaard, H., Twyman, R. E. & Schmidt, D. New avenues for anti-epileptic drug discovery and development. *Nat. Rev. Drug Discov.* **12,** 757–776 (2013).
3. Luszczki, J. J. Third-generation antiepileptic drugs: mechanisms of action, pharmacokinetics and interactions. *Pharmacol. Rep.* **61,** 197–216 (2009).
4. Kullmann, D. M., Schorge, S., Walker, M. C. & Wykes, R. C. Gene therapy in epilepsy-is it time for clinical trials? *Nat. Rev. Neurol.* **10,** 300–304 (2014).
5. Snowball, A. & Schorge, S. Changing channels in pain and epilepsy: Exploiting ion channel gene therapy for disorders of neuronal hyperexcitability. *FEBS Lett.* **589,** 1620–1634 (2015).
6. Barrese, V. *et al.* Neuronal potassium channel openers in the management of epilepsy: role and potential of retigabine. *Clin. Pharmacol.* **2,** 225–236 (2010).
7. Gunthorpe, M. J., Large, C. H. & Sankar, R. The mechanism of action of retigabine (ezogabine), a first-in-class K+ channel opener for the treatment of epilepsy. *Epilepsia* **53,** 412–424 (2012).
8. Main, M. J. *et al.* Modulation of KCNQ2/3 potassium channels by the novel anticonvulsant retigabine. *Mol. Pharmacol.* **58,** 253–262 (2000).
9. Yue, C. & Yaari, Y. KCNQ/M channels control spike afterdepolarization and burst generation in hippocampal neurons. *J. Neurosci.* **24,** 4614–4624 (2004).
10. Biervert, C. *et al.* A potassium channel mutation in neonatal human epilepsy. *Science* **279,** 403–406 (1998).
11. Singh, N. A. *et al.* A novel potassium channel gene, KCNQ2, is mutated in an inherited epilepsy of newborns. *Nat. Genet.* **18,** 25–29 (1998).
12. Soldovieri, M. V., Miceli, F. & Taglialatela, M. Driving with no brakes: molecular pathophysiology of kv7 potassium channels. *Physiology.* (*Bethesda.*) **26,** 365–376 (2011).
13. Miceli, F. *et al.* Genotype-phenotype correlations in neonatal epilepsies caused by mutations in the voltage sensor of K(v)7.2 potassium channel subunits. *Proc. Natl. Acad. Sci. USA* **110,** 4386–4391 (2013).
14. Miceli, F. *et al.* A novel KCNQ3 mutation in familial epilepsy with focal seizures and intellectual disability. *Epilepsia* **56,** e15–e20 (2015).
15. Miceli, F. *et al.* Early-onset epileptic encephalopathy caused by gain-of-function mutations in the voltage sensor of Kv7.2 and Kv7.3 potassium channel subunits. *J. Neurosci.* **35,** 3782–3793 (2015).
16. Wuttke, T. V., Seebohm, G., Bail, S., Maljevic, S. & Lerche, H. The new anticonvulsant retigabine favors voltage-dependent opening of the Kv7.2 (KCNQ2) channel by binding to its activation gate. *Mol. Pharmacol.* **67,** 1009–1017 (2005).
17. Schenzer, A. *et al.* Molecular determinants of KCNQ (Kv7) K+ channel sensitivity to the anticonvulsant retigabine. *J. Neurosci.* **25,** 5051–5060 (2005).
18. Lange, W. *et al.* Refinement of the binding site and mode of action of the anticonvulsant Retigabine on KCNQ K+ channels. *Mol. Pharmacol.* **75,** 272–280 (2009).
19. Kim, R. Y. *et al.* Atomic basis for therapeutic activation of neuronal potassium channels. *Nat. Commun.* **6,** 8116 (2015).
20. Haut, S. R. & Lipton, R. B. Migraine and epilepsy: progress towards preemptive therapy. *Epilepsy Behav.* **28,** 241–242 (2013).
21. Hayashi, H., Iwata, M., Tsuchimori, N. & Matsumoto, T. Activation of peripheral KCNQ channels attenuates inflammatory pain. *Mol. Pain* **10,** 15 (2014).
22. Kalappa, B. I. *et al.* Potent KCNQ2/3-specific channel activator suppresses *in vivo* epileptic activity and prevents the development of tinnitus. *J. Neurosci.* **35,** 8829–8842 (2015).
23. Cao, Y. *et al.* Rescue of homeostatic regulation of striatal excitability and locomotor activity in a mouse model of Huntington's disease. *Proc. Natl. Acad. Sci. USA* **112,** 2239–2244 (2015).
24. Rekling, J. C. Neuroprotective effects of anticonvulsants in rat hippocampal slice cultures exposed to oxygen/glucose deprivation. *Neurosci. Lett.* **335,** 167–170 (2003).
25. Boscia, F., Annunziato, L. & Taglialatela, M. Retigabine and flupirtine exert neuroprotective actions in organotypic hippocampal cultures. *Neuropharmacol.* **51,** 283–294 (2006).
26. Barrese, V., Taglialatela, M., Greenwood, I. A. & Davidson, C. Protective role of Kv7 channels in oxygen and glucose deprivation-induced damage in rat caudate brain slices. *J. Cereb. Blood Flow Metab.* **35,** 1593–1600 (2015).
27. Treven, M. *et al.* The anticonvulsant retigabine is a subtype selective modulator of GABAA receptors. *Epilepsia* **56,** 647–657 (2015).
28. Garin, S. T. *et al.* Blue-gray mucocutaneous discoloration: a new adverse effect of ezogabine. *JAMA Dermatol.* **150,** 984–989 (2014).
29. Clark, S., Antell, A. & Kaufman, K. New antiepileptic medication linked to blue discoloration of the skin and eyes. *Ther. Adv. Drug Saf.* **6,** 15–19 (2015).
30. Jia, Q. *et al.* Activation of epidermal growth factor receptor inhibits KCNQ2/3 current through two distinct pathways: membrane PtdIns(4,5)P2 hydrolysis and channel phosphorylation. *J. Neurosci.* **27,** 2503–2512 (2007).
31. Abbott, G. W. KCNE2 and the K (+) channel: the tail wagging the dog. *Channels (Austin.)* **6,** 1–10 (2012).
32. Tinel, N. *et al.* M-type KCNQ2-KCNQ3 potassium channels are modulated by the KCNE2 subunit. *FEBS Lett.* **480,** 137–141 (2000).

33. McCrossan, Z. A. & Abbott, G. W. The MinK-related peptides. *Neuropharmacol.* **47,** 787–821 (2004).
34. Zhou, P. *et al.* Phosphatidylinositol 4,5-bisphosphate alters pharmacological selectivity for epilepsy-causing KCNQ potassium channels. *Proc. Natl. Acad. Sci. USA* **110,** 8726–8731 (2013).
35. Bocksteins, E. & Snyders, D. J. Electrically silent Kv subunits: their molecular and functional characteristics. *Physiology* (*Bethesda*) **27,** 73–84 (2012).
36. Mohapatra, D. P. *et al.* Regulation of intrinsic excitability in hippocampal neurons by activity-dependent modulation of the KV2.1 potassium channel. *Channels* (*Austin.*) **3,** 46–56 (2009).
37. Liu, P. W. & Bean, B. P. Kv2 channel regulation of action potential repolarization and firing patterns in superior cervical ganglion neurons and hippocampal CA1 pyramidal neurons. *J. Neurosci.* **34,** 4991–5002 (2014).
38. Porter, R. J., Partiot, A., Sachdeo, R., Nohria, V. & Alves, W. M. Randomized, multicenter, dose-ranging trial of retigabine for partial-onset seizures. *Neurology* **68,** 1197–1204 (2007).
39. Brodie, M. J. *et al.* Efficacy and safety of adjunctive ezogabine (retigabine) in refractory partial epilepsy. *Neurology* **75,** 1817–1824 (2010).
40. French, J. A. *et al.* Randomized, double-blind, placebo-controlled trial of ezogabine (retigabine) in partial epilepsy. *Neurology* **76,** 1555–1563 (2011).
41. Orhan, G., Wuttke, T. V., Nies, A. T., Schwab, M. & Lerche, H. Retigabine/Ezogabine, a KCNQ/K(V)7 channel opener: pharmacological and clinical data. *Expert. Opin. Pharmacother.* **13,** 1807–1816 (2012).
42. Biton, V., Gil-Nagel, A., Brodie, M. J., Derossett, S. E. & Nohria, V. Safety and tolerability of different titration rates of retigabine (ezogabine) in patients with partial-onset seizures. *Epilepsy Res.* **107,** 138–145 (2013).
43. Misonou, H., Mohapatra, D. P. & Trimmer, J. S. Kv2.1: a voltage-gated k+ channel critical to dynamic control of neuronal excitability. *Neurotoxicology* **26,** 743–752 (2005).
44. Yang, S. N. *et al.* Ionic mechanisms in pancreatic beta cell signaling. *Cell Mol. Life Sci.* **71,** 4149–4177 (2014).
45. Murakoshi, H. & Trimmer, J. S. Identification of the Kv2.1 K^+ channel as a major component of the delayed rectifier K^+ current in rat hippocampal neurons. *J. Neurosci.* **19,** 1728–1735 (1999).
46. Speca, D. J. *et al.* Deletion of the Kv2.1 delayed rectifier potassium channel leads to neuronal and behavioral hyperexcitability. *Genes Brain Behav.* **13,** 394–408 (2014).
47. Antonucci, D. E., Lim, S. T., Vassanelli, S. & Trimmer, J. S. Dynamic localization and clustering of dendritic Kv2.1 voltage-dependent potassium channels in developing hippocampal neurons. *Neurosci.* **108,** 69–81 (2001).
48. O'Connell, K. M. & Tamkun, M. M. Targeting of voltage-gated potassium channel isoforms to distinct cell surface microdomains. *J. Cell Sci.* **118,** 2155–2166 (2005).
49. O'Connell, K. M., Loftus, R. & Tamkun, M. M. Localization-dependent activity of the Kv2.1 delayed-rectifier K+ channel. *Proc. Natl. Acad. Sci. USA* **107,** 12351–12356 (2010).
50. Fox, P. D., Loftus, R. J. & Tamkun, M. M. Regulation of Kv2.1 K(+) conductance by cell surface channel density. *J. Neurosci.* **33,** 1259–1270 (2013).
51. Fox, P. D. *et al.* Induction of stable ER-plasma-membrane junctions by Kv2.1 potassium channels. *J. Cell Sci.* **128,** 2096–2105 (2015).
52. Deutsch, E. *et al.* Kv2.1 cell surface clusters are insertion platforms for ion channel delivery to the plasma membrane. *Mol. Biol. Cell* **23,** 2917–2929 (2012).
53. Misonou, H. *et al.* Bidirectional activity-dependent regulation of neuronal ion channel phosphorylation. *J. Neurosci.* **26,** 13505–13514 (2006).
54. Cerda, O. & Trimmer, J. S. Activity-dependent Phosphorylation of Neuronal Kv2.1 Potassium Channels by CDK5. *J. Biol. Chem.* **286,** 28738–28748 (2011).
55. Misonou, H. *et al.* Regulation of ion channel localization and phosphorylation by neuronal activity. *Nat. Neurosci.* **7,** 711–718 (2004).
56. Pal, S., Hartnett, K. A., Nerbonne, J. M., Levitan, E. S. & Aizenman, E. Mediation of neuronal apoptosis by Kv2.1-encoded potassium channels. *J. Neurosci.* **23,** 4798–4802 (2003).
57. Shah, N. H. & Aizenman, E. Voltage-gated potassium channels at the crossroads of neuronal function, ischemic tolerance, and neurodegeneration. *Transl. Stroke Res.* **5,** 38–58 (2014).
58. Pal, S. K., Takimoto, K., Aizenman, E. & Levitan, E. S. Apoptotic surface delivery of K+ channels. *Cell Death. Differ.* **13,** 661–667 (2006).
59. Zaks-Makhina, E., Kim, Y., Aizenman, E. & Levitan, E. S. Novel neuroprotective K+ channel inhibitor identified by high-throughput screening in yeast. *Mol. Pharmacol.* **65,** 214–219 (2004).
60. Boulet, I. R., Raes, A. L., Ottschytsch, N. & Snyders, D. J. Functional effects of a KCNQ1 mutation associated with the long QT syndrome. *Cardiovasc. Res.* **70,** 466–474 (2006).
61. Jensen, C. S. *et al.* Specific sorting and post-Golgi trafficking of dendritic potassium channels in living neurons. *J. Biol. Chem.* **289,** 10566–10581 (2014).
62. Stas, J. I., Bocksteins, E., Labro, A. J. & Snyders, D. J. Modulation of Closed-State Inactivation in Kv2.1/Kv6.4 Heterotetramers as Mechanism for 4-AP Induced Potentiation. *PLoS. ONE.* **10,** e0141349 (2015).

Acknowledgements

We would like to thank Zoë Anderson-Jenkins for linguistic corrections. This work was supported by the Ph.D fellowships FWO-11M0514N and FWO-11M0516N to Jeroen I. Stas, the postdoctoral fellowships FWO-1291913N and FWO-1291916N to Elke Bocksteins and FWO-G.0449.11 and FWO-G.0433.12 to Dirk J. Snyders from the Research Foundation–Flanders (FWO), Belgium. Camilla S. Jensen was supported by the Lundbeck Foundation and the Carlsberg Foundation, Denmark.

Author Contributions

Performed electrophysiological experiments on HEK293 cells and hippocampal neurons: J.I.S. Isolated and cultured the rat hippocampal neurons: J.I.S., E.B. and C.S.J. Contributed to the study design: J.I.S. and E.B. Contributed to the manuscript writing: J.I.S., E.B., C.S.J., N.S. and D.J.S.

Additional Information

Supplementary information accompanies this paper at http://www.nature.com/srep

Competing financial interests: The authors declare no competing financial interests.

How to cite this article: Stas, J. I. *et al.* The anticonvulsant retigabine suppresses neuronal K_V 2-mediated currents. *Sci. Rep.* **6**, 35080; doi: 10.1038/srep35080 (2016).